

## Investigations on structural, optical, and AC conductivity of Polyaniline/Manganese Dioxide nanocomposites

Subbiah Chelladurai Vella Durai<sup>1,\*</sup>, Esakkimuthu Kumar<sup>2</sup>, Durairaj Muthuraj<sup>3</sup>,  
Vethamanickam Bena Jothy<sup>4</sup>

<sup>1</sup>Department of Physics, JP College of Arts and Science, Agarakattu, Tenkasi - 627852, Tamil Nadu, India.

<sup>2</sup>School of Science, Tamil Nadu Open University, Chennai-600015. Tamil Nadu, India.

<sup>3</sup>PG and Research Department of Physics, the M.D.T Hindu College, Tirunelveli -627010. Tamil Nadu, India.

<sup>4</sup>Department of Physics and Research Center, Women's Christian College, Nagarcoil -629001. Tamil Nadu, India.

Received 08 February 2019;

revised 28 April 2019;

accepted 05 May 2019;

available online 08 May 2019

### Abstract

A Polyaniline/Manganese dioxide (PANI/MnO<sub>2</sub>) nanocomposite contains five weight percentages of MnO<sub>2</sub>. It has been successfully prepared by in situ polymerization. The structural, optical, and conductivity of nanocomposites remain relative to changes with respect to the weight percentage of MnO<sub>2</sub>. The structural, morphological, optical, and electrical conductivity investigation of pure MnO<sub>2</sub>, pure PANI, and nanocomposites were done with powder XRD, HRTEM, SEM, FT-IR, UV and Impedance spectra. XRD results of the PANI/MnO<sub>2</sub> nanocomposites say that the crystalline structure is converted into a very less crystalline structure due to the incorporation of MnO<sub>2</sub> which is inside PANI chain. The HRTEM and SEM images are confirmed to the nanocomposite formation, morphology studies and also supported to the XRD results. From the optical spectra, MnO<sub>2</sub> nanoparticles have been impressed in the surface of PANI. It works as the compensator in the formation of nanocomposites. UV spectral analysis reveals that the absorption of MnO<sub>2</sub> modifies the absorption wavelength of under visible light in whole range. The absorption wavelength of nanocomposites is 288 nm and 337 nm. AC electrical conductivity of the prepared nanocomposites from impedance spectroscopy was carried out and compared with pure materials. The AC conductivity of as-prepared nanocomposites has been analyzed in the range of 298 K to 423 K. The AC conductivity of nanocomposites varies depending upon a change of logarithmic frequency.

**Keywords:** Conductivity; Nanoparticles; Polyaniline; Polymerization; Surface.

### How to cite this article

Chelladurai Vella Durai S, Kumar E, Muthuraj D, Bena Jothy V. Investigations on structural, optical, and AC conductivity of Polyaniline/Manganese Dioxide nanocomposites. *Int. J. Nano Dimens.*, 2019; 10 (4): 410-416.

## INTRODUCTION

As nanocomposites are used in many effective applications, its growth is very high in twenty-first century [1]. Since nanocomposite has unique properties, there was much attraction all over the world towards unique properties in researcher. Nanocomposite is the most promising application field of recent research and technical applications. Combination of the desired properties, materials, and composites increases their high potential applications in futures [2]. The selection of the

ingredients of nanocomposites like polymer/metal oxide composite leads to the important application of considerable materials [3]. As physical and chemical properties are good, much interest is shown on nanocomposites material in this research [4]. Some electric conducting polymer has been conjugated in between the chemical bands and monomers, and beneath special doping condition. The conductivity of the polymer electron has taken care [5]. This type of polymer shows that the new materials are manufactured for different applications. The above

\* Corresponding Author Email: [duraipree@gmail.com](mailto:duraipree@gmail.com)

mentioned behaviour are seen in polyaniline (PANI). Metal oxides occupied a principle role in many fields of physics and material science. The metal oxide has easily embraced a structural behaviour with an electronic structure. So, the insulator, semiconductor and metallic behaviour are explained easily [6]. This phenomenon has been found in manganese oxides and chemical applications have long been used as technological importance. However,  $\text{MnO}_2$  exhibits an electrochemical capacitance in comparison with another oxidation [7,8]. PANI/ $\text{MnO}_2$  nanocomposites were prepared in order to increase the performance of Manganese dioxide [9-11]. Among these polymers, PANI/ Manganese dioxide nanocomposites have many applications because the capacitance of these nanocomposites was increased compared with that of pure  $\text{MnO}_2$  due to the high conductivity of PANI and the correlation effect between PANI and  $\text{MnO}_2$  [12]. Preparation and studies of PANI/ $\text{MnO}_2$  nanocomposites have attracted much attention due to small amount and environment friendliness of the active mangle and also due to a good coating layer to restrain  $\text{MnO}_2$  from dissolution in acidic environment [11]. PANI can be prepared using many routes [13]. Oxidation methods of aniline are easy to prepare via simple electrochemical or chemical [14]. The wide range applications of PANI are anti corrosion coating, sensors and batteries [15]. It is known from many research articles that the preparation of PANI/Manganese dioxide nanocomposites was used in electrochemical method. However, it's known that no work has been done on prepared nanocomposites for PANI/Manganese dioxide via in situ polymerization method with HCl and Ammonium per sulphate as oxidant. In this paper, the initial work is described and it has been utilized for optical and structural study of PANI/ $\text{MnO}_2$  nanocomposite.

## MATERIALS AND METHODS

### Chemicals

Chemicals, used in this work, are aniline, Ammonium per sulphate, HCl,  $\text{MgSO}_4$ ,  $\text{MnC}_2\text{O}_4$ , NaOH and deionized water. These chemicals were purchased from MERCK (analytical reagent grade) and ammonium per sulphate was purchased from RANBAXY (analytical reagent).

### Synthesis

#### Manganese Dioxide Nanoparticles Preparation

Two varied salts ( $\text{MnSO}_4$  and  $\text{MnC}_2\text{O}_4$ ) have varied molarities are added and stirred at  $60^\circ\text{C}$  in one hr. While stirring, sodium hydroxide was

mixed with solution to reach 12 pH values. The stirring was continued for one hour at  $60^\circ\text{C}$ . Then the stirring solution was kept at  $30^\circ\text{C}$  in oven and kept out for two hr to become cool. Synthesized brown precipitate was filtered with de-ionized water and cleaned with ethanol. Brown colour precipitates were dried for three days at normal temperature.

#### PANI nanoparticles preparation

4.5 ml aniline was injected into 70 ml of hydrochloric solution. After 6 hours, preparations of 4.5 gram of ammonium per sulphate were dissolved in twenty ml de-ionized  $\text{H}_2\text{O}$  and it was mixed into prepared solution with constant stirring. The polymerization was developed to proceed for three hours at  $60^\circ\text{C}$ . The reaction solution was filtered, washed with 2M HCl and de-ionized  $\text{H}_2\text{O}$ . Afterwards, it is dried at  $90^\circ\text{C}$  in vacuum for 1 day to get a green powder.

#### PANI / $\text{MnO}_2$ nanocomposite (Five Weight Percentage) preparation

Five weight percentages of Polyaniline/ Manganese dioxide nanocomposites was synthesized as follows: 4.5 ml aniline was injected into 70 ml of 2M of HCl which contains  $\text{MnO}_2$  nanoparticles of 0.09g (5 weight percentage). After six hrs, 4.5 g of APS was taken and dissolved in 20ml deionized water. Here, the first prepared solution is mixed to drop wise and stirred at  $60^\circ\text{C}$  for 30 min. The reaction solution was filtered, washed with two molarity HCl and deionized water. Afterwards, it is dried at  $100^\circ\text{C}$  in vacuum for two days to obtain a green powder.

### Experimental

The Powder XRD of the prepared samples were characterized using powder X-ray diffractometer (XPRT-PRO using  $\text{CuK}\alpha 1$ ,  $\lambda=0.1540$  nm radiations). The sample was scattered by the angle  $2\theta$  values as  $10^\circ$  to  $80^\circ$ . The formation of nanocomposites carried out the High Resolution Transmission Electron Microscope using JOEL JEM 2000 and Scanning Electron Microscope using VEGA3 TESCAN. The powder sample was recorded by FT-IR spectrum using FTIR (JASCO FTIR-4100) in range of wavelength as  $399.1927-4000.6047\text{cm}^{-1}$ . The sample was recorded by optical spectrum using UV Visible spectroscopy (UV-2600) in range of wave number as  $200-1200\text{cm}^{-1}$ . The AC conductivity was recorded in the frequency range of 1 Hz to 8 MHz

by impedance spectroscopy (Zahner zennium IM6 meter).

**RESULTS AND DISCUSSION**

*Structural Analysis*

*XRD Studies*

The Powder X-Ray diffraction studies were used to analyse the structure and crystalline behaviour of the PANI, MnO<sub>2</sub> and PANI/MnO<sub>2</sub> nanocomposites. Fig. 1(a, b, and c) shows powder X-ray diffraction of polyaniline, manganese dioxide particles, and 5 wt % PANI/MnO<sub>2</sub> nanocomposites. The manganese dioxide nanoparticles indicate that it evinces a broad diffraction peaks occurred between 25° to 60° (Fig. 1(b)) and it was confirmed to crystalline behavior [16]. The MnO<sub>2</sub> peaks of 2θ = 50°, 42°, 39°, 36°, 28°, 25° are the characteristics. The MnO<sub>2</sub> nanoparticles were identified using

permanent JCPDS file number 44-0141. MnO<sub>2</sub> has a tetragonal structure which is nice agreement with some research articles [16]. The MnO<sub>2</sub> parameters of unit cell are a=9.784Å, b=9.784Å and c=2.863Å [19]. The MnO<sub>2</sub> nanoparticles boundary size is 26 to 30 nm in some research papers [17, 18]. In these experiments, average crystallite diameter of manganese dioxide is 20 nm and is found by Debye Scherrer’s formula (Crystallite size D = 0.9λ/β Cosθ). From the Fig. 1(a), PANI also shows the broad diffraction peaks in the range between of 10° to 45°, it also confirms the behavior of crystalline. The PANI peaks of 2θ = 33°, 28°, 22°, 11° are the characteristics. The PANI nanoparticles were identified using permanent JCPDS file numbers 53-1891. The particle grain size is 8 to 9 nm in few research papers [20]. The powder X-ray diffraction pattern of (5wt%)

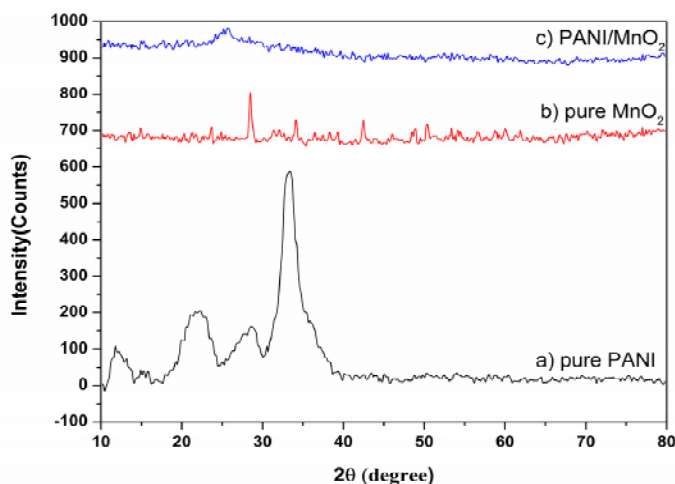


Fig. 1. X-ray diffraction pattern of (a) pure PANI, (b) pure MnO<sub>2</sub> and (c) Five weight percentage of MnO<sub>2</sub>/PANI nanocomposite.

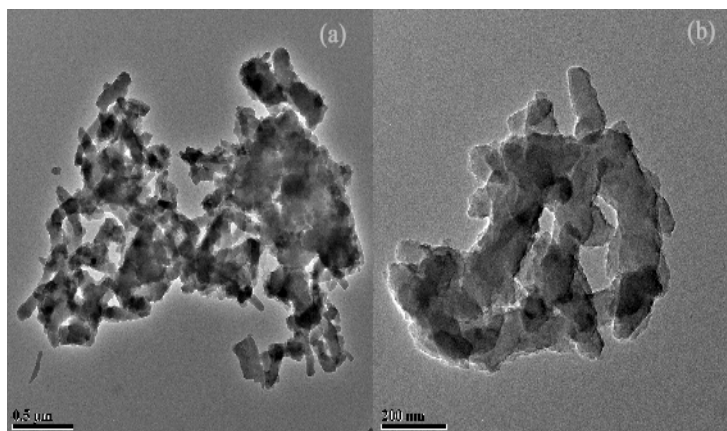


Fig. 2 (a and b). HRTEM image for five weight percentage of PANI/MnO<sub>2</sub> nanocomposites.

PANI/MnO<sub>2</sub> nanocomposites figure is shown in 1(c). In the presence of MnO<sub>2</sub> in PANI, crystalline behaviour of nanocomposites was fully changed. As expected, 5wt% of MnO<sub>2</sub> has affected the PANI chain while they may make changes in the properties of conducting polymer. From the Fig. 1c, nanocomposites do not have any broad peaks in the range between 10° to 80°, and it confirms the interaction of MnO<sub>2</sub> and PANI by the formation of nanocomposites. These results show that the 5 wt% of PANI/MnO<sub>2</sub> nanocomposites is decreasing the crystallite nature. The nanocomposites structural behaviour has been confirmed by HRTEM and SEM analysis.

#### High Resolution Transmission Electron Microscope (HRTEM)

Fig. 2 (a and b) shows the HRTEM images of PANI/MnO<sub>2</sub> nanocomposite. The inset MnO<sub>2</sub> nanoparticles show figures in black. The MnO<sub>2</sub>

nanoparticles were embedded in the PANI matrix forming core shell structure; it is shown in Fig. 2. The HRTEM image indicates that the nanocomposites particles have uniform dispersion with irregular shaped morphology. The grain boundaries in the strip could not be found correctly. However it is found that the edges of very small particles connect to large particles. So it should be noted that the size of the MnO<sub>2</sub> islands is not uniform. It confirms and supports the XRD analysis.

#### Scanning Electron Microscope (SEM)

Morphologies of the PANI/MnO<sub>2</sub> nanocomposites were examined using SEM techniques. Fig. 3 (a and b) represents the SEM micrographs of the PANI/MnO<sub>2</sub> nanocomposites. Manganese dioxide is intercalated between polyaniline layers and is maintained. The SEM image of PANI/MnO<sub>2</sub> nanocomposite is composed of more than two nanoparticles which are connected to each other

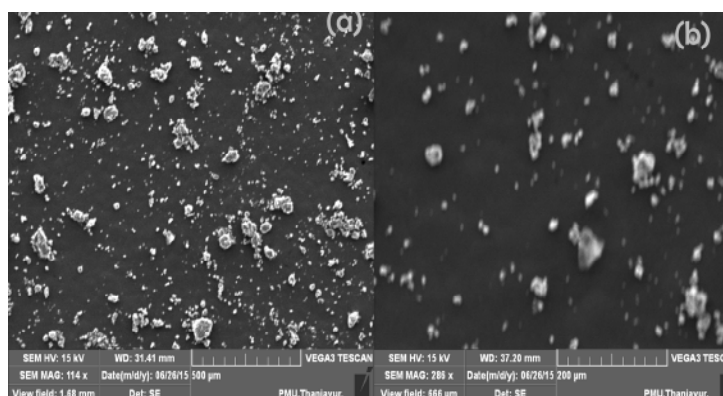


Fig. 3 (a and b). SEM images for five weight percentage of PANI/MnO<sub>2</sub> nanocomposites.

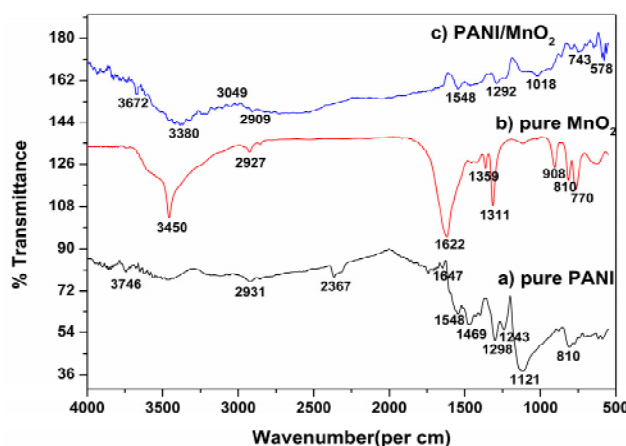


Fig. 4. FTIR spectra of (a) pure PANI, (b) pure MnO<sub>2</sub> and (c) Five weight percentage of PANI/ MnO<sub>2</sub> nanocomposite.

resulting in a porous structure. It also confirms the results of XRD analysis.

#### Optical Analysis

##### FTIR Spectroscopy

Structural information and functional group was identified using FTIR spectroscopy of five weight percentage in PANI/MnO<sub>2</sub> nanocomposite. Fig. 4(a) shows that the peaks at 2931, 2367, 1647, 1548, 1469, 1298, 1121 and 810 cm<sup>-1</sup> are pure PANI. Fig. 4(b) shows that the peaks at 3450, 2927, 1622, 1311, 908, 810 and 770 cm<sup>-1</sup> are pure manganese dioxide nanoparticles. Fig. 4(c) shows that the peaks at 3672, 1548, 1292, 1018 and 578 cm<sup>-1</sup> are five weight percentages of PANI/MnO<sub>2</sub> nanocomposites. In between the wavenumber of 499 cm<sup>-1</sup> to 899 cm<sup>-1</sup>, some absorption bands are placed. Manganese dioxide is the characteristic band of Mn-O bending vibration of octahedral [21]. The manganese dioxide nanoparticles show that wide peak at 3450 cm<sup>-1</sup> and were associated to the adsorbed H<sub>2</sub>O molecule. The peaks 1,292 cm<sup>-1</sup> is C-N stretching and 1,292 cm<sup>-1</sup> is C-H bending of PANI [22]. The conductivity of PANI at 1121 cm<sup>-1</sup> is a very strong peak and the degree of delocalization of electrons was measured. The very weak and small peak 810 cm<sup>-1</sup> is very near to C-H out of plane bonding in benzenoid ring of PANI chain. Fig. 4(c) clearly shows that the 5 wt % of PANI/MnO<sub>2</sub> nanocomposites was compared to pure PANI and pure MnO<sub>2</sub>. The weak peak at 3049 cm<sup>-1</sup> is shows that the N-H stretching region of nanocomposites (curves c). Comparatively, this

peak was very weak in the PANI (curve a). The small peak 578 cm<sup>-1</sup> indicates the PANI of C-N-C bonding mode of aromatic ring. In nanocomposites peak, 743 cm<sup>-1</sup> is C-C and C-H bonding in benzenoid ring, 1292 cm<sup>-1</sup> is C-N stretching of benzenoid ring, 3380 cm<sup>-1</sup> is vibration band of -OH. All these are indicating as a PANI chain. All the other peaks 3672, 1548 and 1018 cm<sup>-1</sup> are shifted, and to near of MnO<sub>2</sub> peaks. Formation of nanocomposites and functional group of nanocomposites have confirmed from the figures.

##### UV - Visible Spectroscopy

Fig. 5(a, b and c) shows UV analysing of pure PANI, Pure MnO<sub>2</sub> and five weight percentage PANI/MnO<sub>2</sub> nanocomposites synthesized as a function of wavelength. The normal temperature UV spectra of Polyaniline/Manganese dioxide nanocomposites samples were recorded absorption (Fig. 5(c)). The peak at 251 nm (Fig. 5(a)) represents the  $\pi$ - $\pi^*$  electron orbital transition along the backbone of the PANI Chain. As PANI/MnO<sub>2</sub> (five weight percentages, Fig. 5(c)) is combined with PANI and MnO<sub>2</sub>, the peak assigned to the polaron- $\pi^*$  transition of the PANI chains shifted to a higher wavelength area. It indicates the interaction between quinoid rings and nanocomposites as written in some article. Regarding the first change was started at 288 nm, the  $\pi$ - $\pi^*$  electron transition of quinoid ring requires small energy for absorption with the presence of PANI/MnO<sub>2</sub> nanocomposites [23]. The maxima red shifted up to 337 nm for five weight percentage of PANI/

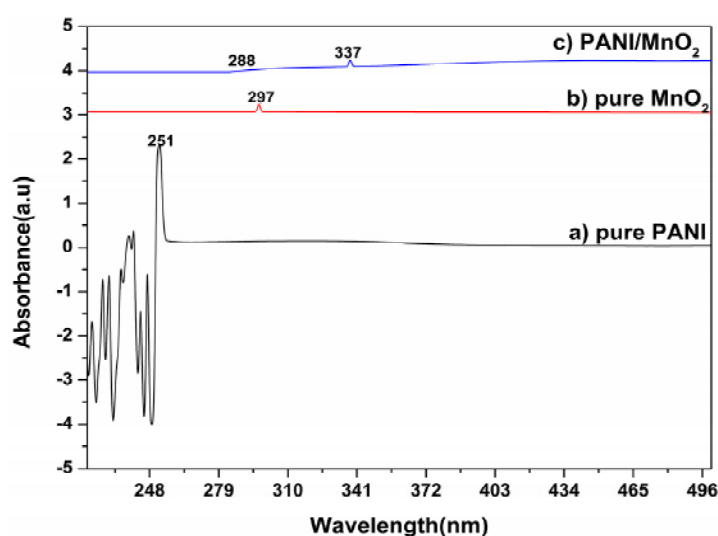


Fig. 5. UV-Visible spectra of (a) pure PANI, (b) pure MnO<sub>2</sub> and (c) Five weight percentage of PANI/ MnO<sub>2</sub> nanocomposite.

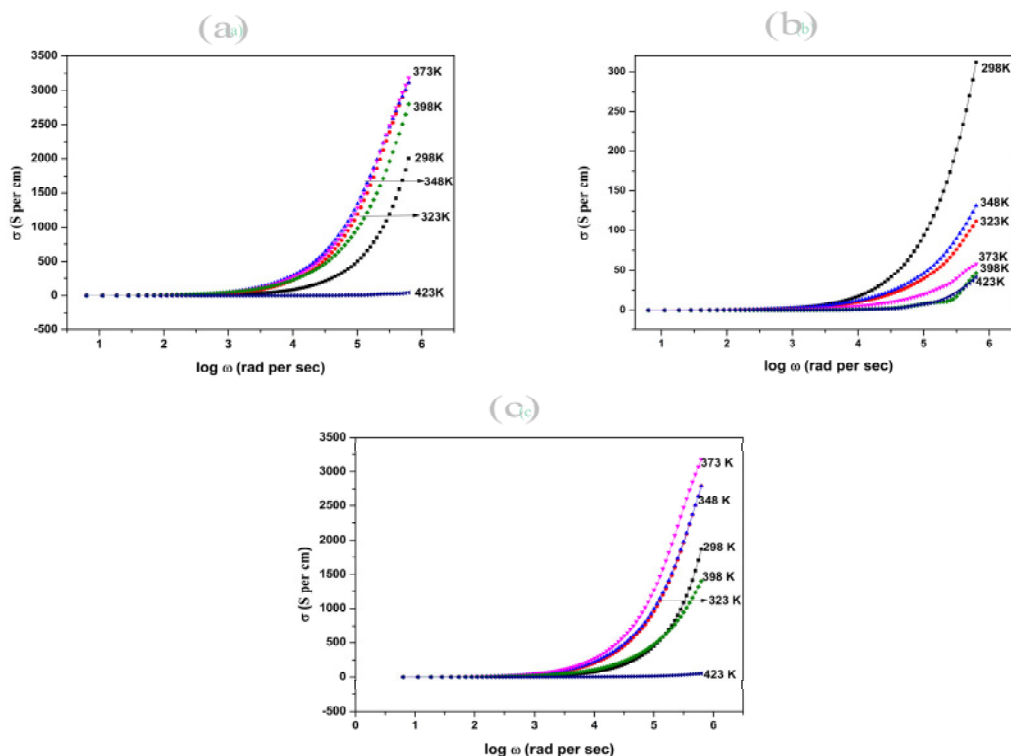


Fig. 6. AC conductivity of (a) pure PANI, (b) pure  $\text{MnO}_2$  and (c) Five weight percentage of PANI/  $\text{MnO}_2$  nanocomposite.

$\text{MnO}_2$  compared to 251 nm and 297 nm of neat PANI and  $\text{MnO}_2$  nanoparticles.

#### Conductivities Analysis

The AC electrical conductive ( $\sigma_{AC}$ ) as a function of frequency at different temperatures are shown in Figs. 6(a, b and c) of pure PANI,  $\text{MnO}_2$  and PANI/ $\text{MnO}_2$  nanocomposites. The conductivity curve of pure nanoparticle and nanocomposites can be classified into three parts: Part I: For pure and composite nanomaterials at all temperature, conductivity is constant in between the frequency ranges of 0.5 to 2.5 rad per sec. The charge carrier motion is rest in these materials for because of constant conductivity. Part II: All materials at all temperature, conductivity slightly increase in between the frequency ranges of 3 to 4.5 rad per sec. The charge carrier motion is lightly flow in these materials because of the increasing conductivity. Part III: For pure PANI (Fig. 6(a)), conductivity is minimum at high temperature and maximum at average temperature. For pure  $\text{MnO}_2$  (Fig. 6(b)), conductivity is maximum at very low temperature, but composite materials, conductivity is totally varied compared to the pure

materials. The conductivity of the PANI/ $\text{MnO}_2$  nanocomposites materials is maximum at normal temperature (Fig. 6(c)). The composite materials conductivity is high to compare with the pure materials.

#### CONCLUSION

In present work, pure and nanocomposites materials were successfully prepared via In Situ Polymerization technique and they were carried out by various studies. Powder X-ray diffraction spectrum predicted the crystalline results in this work. It confirms the nanocomposites with PANI and  $\text{MnO}_2$  nanoparticles. The formation and functional group of the nanocomposites was identified from fourier transform infrared spectra. UV-visible absorption of the all prepared samples, shown, show the absorption peaks at visible region due to  $\text{MnO}_2$  in the polyaniline chain. The impedance spectroscopy studies were successfully carried out and conductivity was discussed between the frequency ranges of 1 Hz to 5 MHz. There are many potential applications of Polyaniline/Manganese dioxide nanocomposites such as in the field of electrode



in different rechargeable batteries, nanoscience and bioscience applications.

#### CONFLICT OF INTEREST

The authors declare that they have no competing interests.

#### REFERENCES

- [1] Camargo P. H. C., Satyanarayana K. G., Wypych F., (2009), Nanocomposites: Synthesis, structure, properties and new application opportunities. *Mater. Res.* 12: 1-39.
- [2] Ali A., Zafar H., Zia M., Haq I., Phull A. R., Ali J. S., Hussain A., (2016), Synthesis, characterization, applications, and challenges of iron oxide nanoparticles. *Nanotechnol. Sci. Appl.* 9: 49-67.
- [3] Li S., Lin M. M., Toprak M. S., Kim D. K., Muhammed M., (2010), Nanocomposites of polymer and inorganic nanoparticles for optical and magnetic applications. *Nano Rev.* 1: 1-19.
- [4] Jancar J., Douglas J. F., Starr F. W., Kumar S. K., Cassagnau P., Lesser A. J., Sternstein S. S., Buehler M. J., (2010), Current issues in research on structure property relationships in polymer nanocomposites. *Polymer.* 51: 3321-3343.
- [5] Bai H., Shi G., (2007), Gas sensors based on conducting polymers. *Sensors.* 7: 267-307.
- [6] Lany S., (2015), Semiconducting transition metal oxides. *J. Phys.: Condens. Matter.* 27: 1-36.
- [7] Singh., Park I. B., Su-Moon., (2015), Synthesis of  $\beta$ -MnO<sub>2</sub> nanowires and their electrochemical capacitive behaviour. *Indian J. Chem.* 54A: 46-51.
- [8] Esam A. G., Mohamed A. M., Amr E. N., Yara A. S., (2017), Cyclic voltammetry of bulk and nano manganese sulfate with Doxorubicin using glassy Carbon electrode. *Int. J. Nano Dimens.* 8: 89-96.
- [9] Tan D. Z. W., Cheng H., Nguyen S. T., Duong H. M., (2014), Controlled synthesis of MnO<sub>2</sub> /CNT nanocomposites for supercapacitor applications. *Mater. Technol.* 29: A107-A113.
- [10] Fanhui M., Xiuling Y., Ye Zh., Pengchao S., (2013), Controllable synthesis of MnO<sub>2</sub>/polyaniline nanocomposite and its electrochemical capacitive property. *Nanoscale Res. Lett.* 8: 179-186.
- [11] Ke-Qiang D., (2009), Cyclic voltammetrically prepared MnO<sub>2</sub>-Polyaniline composite and its electrocatalysis for oxygen reduction reaction (ORR). *J. Chin. Chem. Soc.* 56: 891-897.
- [12] Saadat L., Sadeghvandi F., (2014), Synthesis and study of Polyethylene/Polyaniline/Montmorillonite ductile nano composites properties. *Int. J. Nano Dimens.* 5: 255-265.
- [13] Vivekanandan J., Ponusamy V., Mahudewaran A., Vijayanand P. S., (2011), Synthesis, characterization and conductivity study of polyaniline prepared by chemical oxidative and electrochemical methods. *Archiv. Appl. Sci. Res.* 3: 147-153.
- [14] Deepshika A., Tinku B., (2010), Development of transducer matrices based upon nanostructured conducting polymer for application in biosensors. *Ind. J. Experiment. Biol.* 48: 1053-1062.
- [15] Michira L., Akinyeye R., Somerset E., Klink M. J., Sekota M., Al-Hmed A., Baker P. G. L., Iwuoha E., (2007), Synthesis, characterisation of novel polyaniline nanomaterials and application in amperometric biosensors. *Makromol. Chem. Macromol. Symp. Makromolekulare Chemie.* 255: 57-69.
- [16] Li Y., Wang J., Zhang Y., Banis M. N., Liu J., Geng D., Li R., Sun X., (2012), Facile controlled synthesis and growth mechanisms of flower-like and tubular MnO<sub>2</sub> nanostructures by microwave-assisted hydrothermal method. *J. Colloid Interf. Sci.* 369: 123-128.
- [17] Harish K., Manisha M., Poonam S., (2013), Synthesis and characterization of MnO<sub>2</sub> nanoparticles using Co-precipitation technique. *Int. J. Chem. Chem. Eng.* 3: 155-160.
- [18] Senthilkumar M., Balamurugan V., Jayapragash B. G., (2013), Hydrothermal synthesis of MnO<sub>2</sub> nanoparticles using Teflon lined Autoclave. *Res. J. Pharmac. Biol. Chem. Sci.* 4: 1627-1632.
- [19] Devaraj S., Munichandraiah N., (2007), Electrochemical supercapacitor studies of nanostructured  $\alpha$ -MnO<sub>2</sub> synthesized by microemulsion method and the effect of annealing. *J. Electrochem. Soc.* 154: A80-A88.
- [20] Srinivas C. H., Srinivasu D., Kavitha B., Narsimlu N., Siva Kumar K., (2012), Synthesis and characterization of nano size conducting polyaniline. *IOSR J. Appl. Phys.* 1: 12-15.
- [21] Abuli A., Yang G. H., Okitso K., Zhu J. J., (2014), Synthesis of MnO<sub>2</sub> nanoparticles from sonochemical reduction of MnO<sub>4</sub><sup>-</sup> in water under different pH conditions. *Ultrason. Sonochem.* 21: 1629-1634.
- [22] Shen J., Liu A., Tu Y., Wang H., Jiang R., Ouyang J., Chen Y., (2012), Asymmetric deposition of manganese oxide in single walled carbon nanotube films as electrodes for flexible high frequency response electrochemical capacitors. *Electrochim. Acta.* 78: 122-133.
- [23] Sridevi V., Malathi S., Devi C. S., (2011), Synthesis and characterization of polyaniline/gold nanocomposites. *Chem. Sci. J.* 26: 1-6.